

Design, Modeling, and Characterization of Hot Electron Light Emission and Lasing in Semiconductor Heterostructure-VCSOA with Optical Gain up to 36 dB

Hawro I. Yaba and Faten A. Chaqmaqchee

Department of Physics, Faculty of Science and Health, Koya University, Koya,
Kurdistan Region - F.R. Iraq

Abstract—Vertical-cavity semiconductor optical amplifiers (VCSOAs) are interesting devices for optical communication applications. In this work, we have studied the characteristics of gain spectra and amplifier bandwidth in reflection mode at 1300 nm *GaInNAs/GaAs* hot electron light emission and lasing in semiconductor heterostructure-VCSOA structure using MATLAB program. The device contains 16 $Ga_{0.7}In_{0.3}N_{0.038}As_{0.962}$ multiple quantum wells (QWs) in its intrinsic region; the active region is bounded between eight pairs of *GaAs/AlAs* top distributed Bragg reflectors (DBRs) mirror and 25 pairs of *AlAs/GaAs* bottom DBRs mirror. Simulation results suggest that the resonance cavity of QW of HILLISH-VCSOA is varied with temperature and number of DBRs periods. We compare the relation between the wavelength and gain at a different single-pass gain in both reflection and transmission modes. The highest gain at around 36 dB is observed in reflection mode. Moreover, we calculated the amplifier bandwidth at different periods of top mirror's reflectivity, in which when the peak reflection gains increases, the amplifier bandwidth decreases.

Index Terms—Hot electron, Vertical-cavity semiconductor optical amplifier, *AlAs* DBRs, *GaInNAs/GaAs* QWs, optical characterization.

I. INTRODUCTION

III–V compound semiconductors have aided the development of modern electrical and optoelectronic devices significantly. They offer a wide range of potential uses in nanometer-scale optoelectronics applications (Razeghi, 2000; Chaqmaqchee and Lott, 2020; Lee, et al., 2022). Adding small quantities of nitrogen into III–V alloys have a significant influence on the fundamental band gap (Yu, et al., 2000) and cause a redshift in emission wavelength (Zhao, et al., 2005). This

discovery has applications in technology of dilute III–V nitride semiconductor devices. The bandgap of the *GaInNAs* semiconductor layer can be worked by incorporating N into *InGaAs*; increasing the N concentration in *GaInNAs* reduces the energy gap, resulting in higher refractive index values (Walukiewicz, et al., 1999; Ugan, et al., 2013). As a result, the propensity for the refractive index to grow as the bandgap energy decreases is the same as in traditional III–V semiconductors (Uesugi, K., Morooka, N. and Suemune, I., 1999). The dilute III–V nitrides compound can be used in long-wavelength optoelectronic as local area network and metropolitan area network (Gönül, Köksal and Bakır, 2007).

GaInNAs may be grown pseudomorphically on *GaAs* in the 1.3 μm optical communications window, enabling the utilization of high-quality *Al(Ga)As/GaAs* distributed Bragg reflectors (DBRs) using MatLab program (Abubaker, S.A., 2021; Chaqmaqchee, et al., 2011; Chaqmaqchee, 2021) with possible cost savings over *InP*-based techniques. Vertical cavity surface-emitting lasers (VCSELs) and vertical-cavity semiconductor optical amplifiers (VCSOAs) are closely related and have many of the same advantages. They are probably low-cost devices that can be used instead of in-plane SOAs (Royo, Koda and Coldren, 2002). They have low fiber-coupling losses and low noise figures and can be fabricated into two-dimensional arrays, unlike in-plane SOAs and they allow high-fiber coupling efficiency and are insensitive to polarization (Hepburn, et al., 2005). An important feature of VCSOAs is the narrow signal gain bandwidth, which allows VCSOAs to function as optical filters with gain. The optical gain not only depends on the wavelength of the incidence signal but also on the intensity inside the semiconductor optical amplifier (Kimura, et al., 2003).

The VCSOA (Bjorlin, 2002; Gauss, et al., 2011) can be amended into hot electron light emission and lasing in semiconductor heterostructure (HELLISH)-VCSOA structure, which differs from the HELLISH-VCSEL structure by reducing the number of top DBR layers (Wah and Balkan, 2004; Chaqmaqchee, 2016). HILLISH-VCSOA is a device that utilizes hot carrier transport parallel to the layers of the p–n junction. The junction contains a *GaInNAs/GaAs* quantum well (QW) in the depletion region. Briefly, the electric field



applied along the layers provides heating of the electrons and holes in their respective channels through tunneling and thermionic emission processes (O'Brien, et al., 1999). Because electrons have smaller effective masses and higher motilities, are excited to higher energy levels than holes. Therefore, they have a higher non-equilibrium temperature than the hole. Hot electrons are injected by the main tunneling into the QW, resulting in emitting light at longer wavelengths (Chaqmaqchee, Balkan and Herrero, 2012).

In this work, the influence of temperature on the cavity resonance together with active material bandgap energy of the HELLISH-VCSSOA was studied using MatLab program. We compare the gain spectra in both reflection mode and transmission modes at different single-pass gain. In addition, the amplifier bandwidth as a function of peak reflection gain is calculated at fixed bottom DBR mirrors and different number of top DBR periods.

II. DESIGN, MODELING, AND SIMULATION METHOD

The VCSSOA design is adapted here using MatLab Program to make a *GaN*-based HELLISH-VCSSOA structure, which differs from the HELLISH-VCSEL structure by reducing the number of top DBR layers. The VCSSOA design is shown in Fig. 1a and is optimized at a wavelength of 1300 nm. The active region is arranged with a cavity length of $3\lambda/(2n_c)$ and formed by four $(\text{Ga}_{0.7}\text{In}_{0.3}\text{N}_{0.038}\text{As}_{0.962})\text{GaAs}$ QWs and each stack with another four layers. It is enclosed between two 150 nm thick doped cladding layers Si doped ($n=1\times 10^{17}\text{ cm}^{-3}$) on the bottom side, and C doped ($p=n=1\times 10^{17}\text{ cm}^{-3}$) on the top side and bounded by 25 periods *GaAs/AlAs* bottom DBRs and eight periods *GaAs/AlAs* top DBRs, both DBRs are undoped, except for the first period in each mirror joining the cavity (Balkan, et al., 2000). The use of MQWs, placed at the electric field antinode of $3/2$ cavity length, is done to provide optical gain Fig. 1b. The number of QW can be modified from 3 to 9 according to HELLISH-VCSSOAs design. The most important problem with such devices is the variation of resonance wavelength, which increases with increasing the

number of QWs. Obviously, the maximum photon energy in the device is for a case with 3 QWs which can be found elsewhere (Ghadimi and Ahmadzadeh, 2020).

The gains in reflection mode (G_r) and transmission mode (G_t) operation (Adams, et al., 1985; Bjorlin, et al., 2001) can be calculated using:

$$G_r = \frac{(\sqrt{R_f} - \sqrt{R_b} g_s)^2 + 4\sqrt{R_f R_b} g_s \sin^2 \phi}{(1 - \sqrt{R_b} g_s)^2 + 4\sqrt{R_f R_b} g_s \sin^2 \phi} \quad (1)$$

$$G_t = \frac{(1 - R_f)(1 - R_b) g_s}{(1 - \sqrt{R_b} g_s)^2 + 4\sqrt{R_f R_b} g_s \sin^2 \phi} \quad (2)$$

where, R_f , R_b , and g_s are the reflectivity of the top DBR mirror, the reflectivity of the bottom DBR mirror, and the single-pass gain, respectively.

The QW material gain (g) can be approximated by Piprek, Bjorlin and Bowers, 2001:

$$g = g_0 \ln\left(\frac{N + N_s}{N_r - N_s}\right) \quad (3)$$

where, g_0 , N , N_r , and N_s are the gain coefficient, the QW carrier density, the transparency carrier density concentration, and fitting parameters, respectively.

The gain bandwidth in the reflected and transmitted modes can be given by Bjorlin, et al., 2001; Erol, 2008:

$$\Delta f_r = \frac{c}{\pi n L} \cdot \arcsin \left[4\sqrt{R_f R_b} g_s \left(\frac{1}{(1 - \sqrt{R_f R_b} g_s)^2} - \frac{2}{(\sqrt{R_f} - \sqrt{R_b})^2} \right) \right]^{-1/2} \quad (4)$$

$$\Delta f_t = \frac{c}{\pi n L} \cdot \arcsin \left[\frac{(1 - \sqrt{R_f R_b} g_s)^2}{4\sqrt{R_f R_b} g_s} \right]^{1/2} \quad (5)$$

where, c and L are the velocity of light in vacuum and the cavity length, respectively.

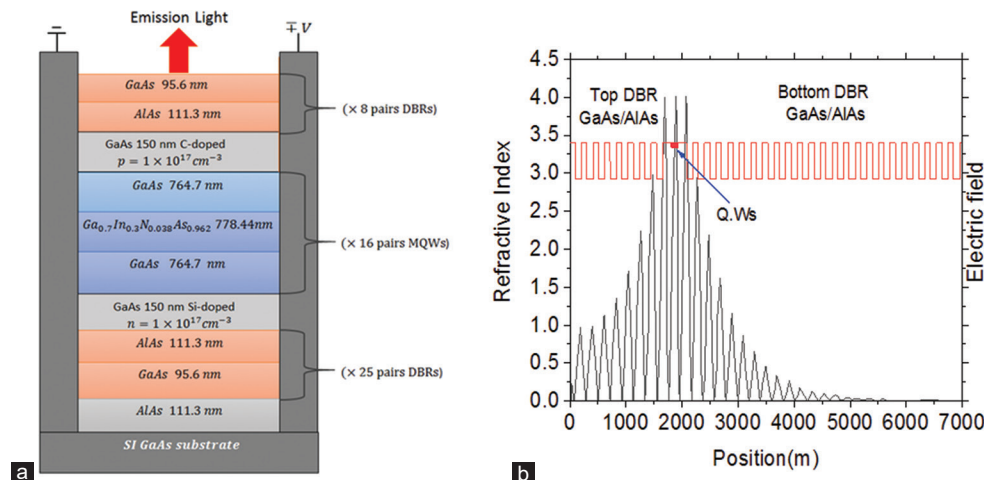


Fig. 1. (a) The schematic diagram illustrates the layer structure of the simple bar HELLISH-VCSSOA, (b) refractive index profile, and the electric field intensity distribution that forms standing.

III. RESULTS AND DISCUSSION

The resonance cavity of HELLISH-VCSOA at various temperatures is shown in Fig. 2. The result shows that when the temperature increases the resonance cavity of the QW shifts to a longer wavelength and the resonance cavity matches with a longer wavelength (1300 nm) due to a higher temperature of 300 K (Su, et al., 2006).

The reflectivity spectra of the *GaInNAs* of HELLISH-VCSOA structure with different periods (8, 11, 14, and 17) are shown in Fig. 3. When the number of top mirrors of *AlAs/GaAs* increased, the reflectivity increased larger than 99% which lead to a high gain bandwidth, whereas low mirror reflectivity causes a lower gain and high saturation power.

The temperature dependence of the cavity resonance together with the *GaInNAs/GaAs* active material bandgap energy curve is plotted in Fig. 4. The behavior of an active medium area is extremely changed with temperature. It shows from the figure that by increasing temperature to 300 K, the material bandgap reduced to ~ 1.005 eV which used for long-

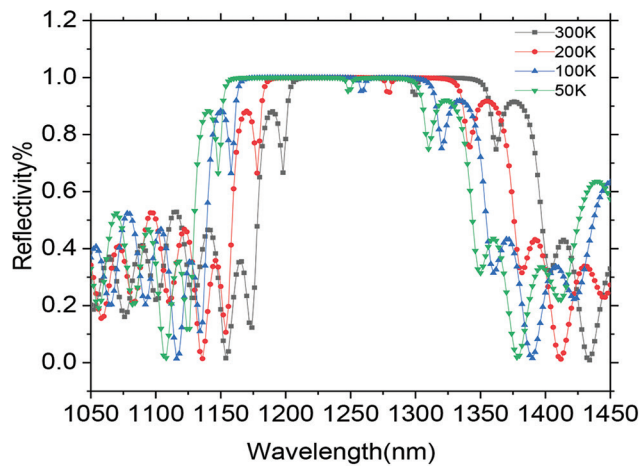


Fig. 2. The resonance cavity of quantum well as a function of different temperatures.

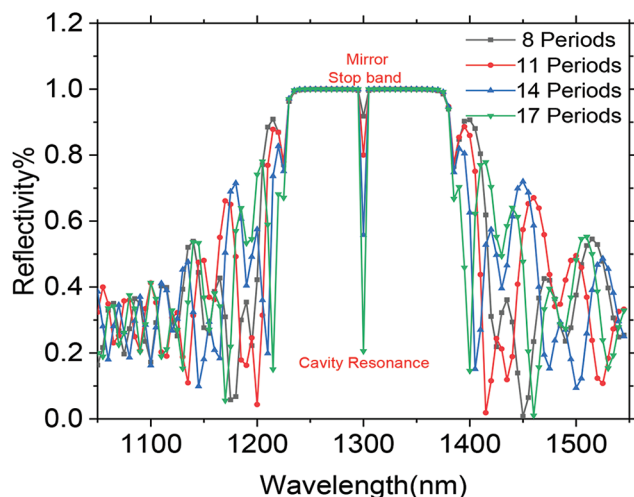


Fig. 3. Reflectivity spectrum for a cavity *GaInNAs* VCISOAs of refractive index ($n=3.34$) placed between varied top DBRs periods and fixed bottom DBRs of 25 periods and cavity resonance at 1300 nm.

wavelength optical communication system. Theoretically, a redshift of the active material peak wavelength at a rate of 0.38 nm/K was predicted, whereas the resonance cavity moves with the temperature at around 0.18 nm/K (Potter and Balkan, 2004).

In Figs. 5 and 6, the gain spectra in reflection and transmission modes for *GaInNAs/GaAs* HELLISH-VCISOAs can be plotted according to Equations 1 and 2 with using various single-pass gains of 1.068, 1.07, 1.072, 1.074, and 1.076. By increasing the single-pass gain from 1.068 to 1.076, the gain spectra are increased from nearly 10.09 dB to 34.838 as shown in Fig. 5 and the gain increased from 10.2 to the as shown in Fig. 6, whereas the bandwidth gets narrower at about 0.0008 nm with increasing single-pass gain. The optical gain in reflection mode is higher than the optical gain in transmission mode under using same single-pass gain. Thus, the higher gain with narrow bandwidth can be useful for filtering application (Chaqmaqchee, et al., 2020). The inset

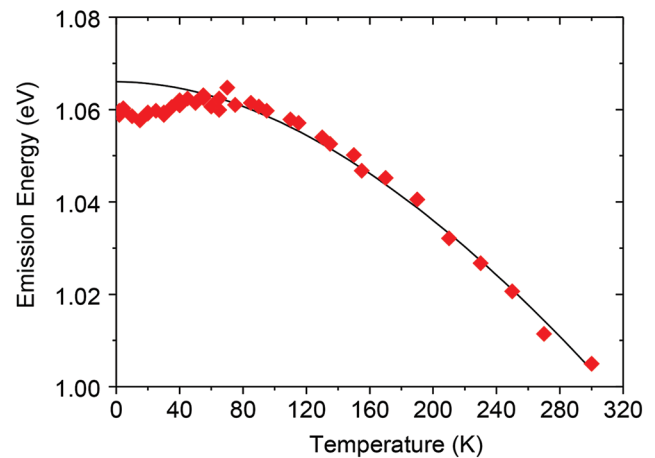


Fig. 4. The red square points represent the calculated temperature dependence of bandgap energy for the device active area (*GaInNAs/GaAs* QW) using the BAC model, whereas the expected cavity resonance position is plotted with a continuous line.

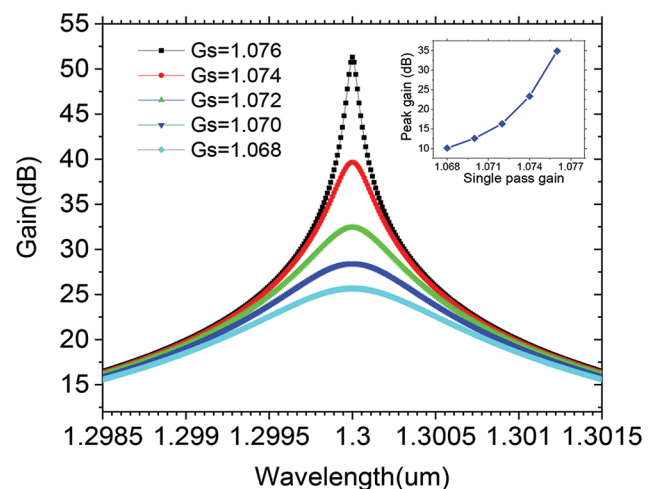


Fig. 5. Reflection VCISOA gains spectra for different G_s values, where $R_f=86.7\%$, $R_o=99.7\%$, and $L_c=3\lambda/2L_o$, the inset shows maximum peak gain versus single-pass gain.

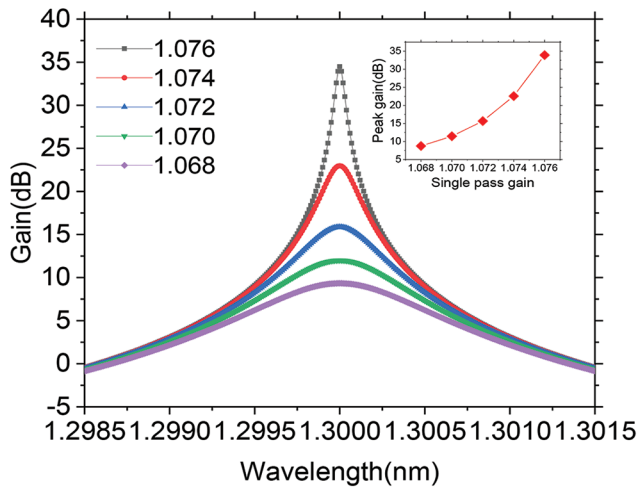


Fig. 6 Transmission VCSOA gains spectra for different G_S values, where $R_f=86.7\%$, $R_b=99.7\%$, and $L_c=3\lambda/2L_c$, the inset shows maximum peak gain versus single-pass gain.

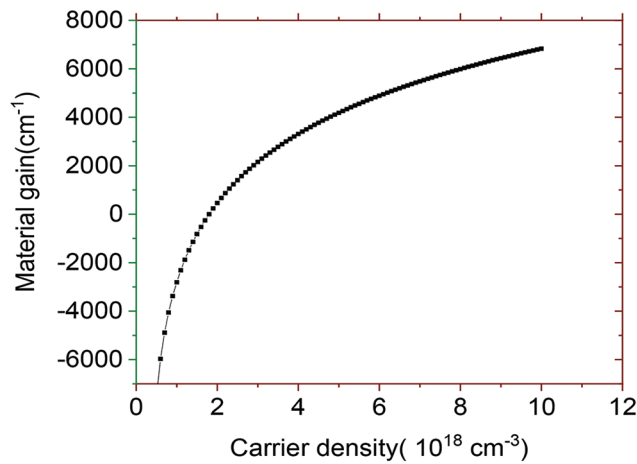


Fig. 7. Material gain versus carrier density curve for *GaInNAs/GaAs* QW active region.

of figures shows the peak gains versus single-pass gain. As a results, the optical gain in reflection mode is about 34.838 dB and in transmission mode is around 34.069 dB.

Fig. 7 illustrates the material gain against the carrier density curve for *GaInNAs/GaAs* QW active region. The gain was calculated using the Equation 3, which recommended a fit parameter of $g_0=3650 \text{ cm}^{-1}$ and transparency carrier density parameter of $N_{tr}=1.8 \times 10^{18} \text{ cm}^{-3}$ (Chaqmaqchee, 2016). The material gain depends on QW of carrier density and its logarithmic inclination, but this model allows for an accurate description of the material gain at low carrier densities. It shows at lower and higher carrier densities, the logarithmic gain model is limited, as it does not calculate the saturation of the material, where the gain cannot be estimated from a linear profile.

Fig. 8 shows amplifier bandwidth versus peak reflection gain for *GaInNAs* of 25 periods of bottom DBR mirrors and different top DBR mirrors reflectivity. The figure shows that when the peak reflection gains increase, the amplifier bandwidth decreases. High gain and shorter amplifier

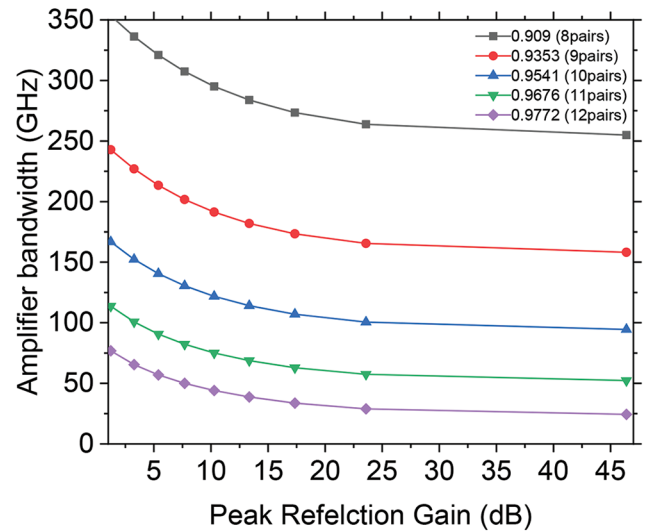


Fig. 8. Amplifier bandwidth versus peak reflection gain using the fixed 25 pairs bottom mirror of 0.99 reflectivity and different pairs of top mirror's reflectivity.

bandwidth are possible because of the increased reflectivity. The small bandwidths are advantageous for filter applications to reduce the noise figure, whereas the larger bandwidths are desirable for devices used in applications with multiple channels (Chaqmaqchee and Balkan, 2012).

IV. CONCLUSION

In this paper, we use the program to investigate and calculating the resonance cavity, the reflectivity of QW, gain, and amplifier bandwidth. The resonance cavity matches the longer wavelength at 300 K without changing the reflectivity. The reflectivity was larger than 99% by increasing the number of periods. The gain in reflection and transmission mode varies proportionally with the single-pass gain. We have achieved high optical gain and narrower bandwidth at around 36 dB with single-pass gains of 1.076, where the gain in reflection mode is higher than the gain in transmission mode for the same single-pass gain. Moreover, the amplifier bandwidth as a function of peak reflection gain for HELLISH-VCSOA at different top DBR periods is measured. High amplifier bandwidth is achieved at around 270 GHz at peak reflection gain of 36 dB with front mirrors reflectivity of $\sim 91\%$.

V. ACKNOWLEDGMENTS

The authors are grateful to the Department of Physics at Koya University for allowing this work.

REFERENCES

- Adams, M.J., Collins, J.V. and Henning, I.D., 1985. Analysis of semiconductor laser optical amplifiers. IEE Proceedings J (Optoelectronics), 132(1), pp.58-63.
- Abubaker Salh, S., 2021. A comparison of top distributed bragg reflector for 1300 nm vertical cavity semiconductor optical amplifiers based on III-V

- compound. *ARO-the Scientific Journal of Koya University*, 9(2), pp.26-29.
- Adams, M.J., Collins, J.V. and Henning, I.D., 1985. Analysis of semiconductor laser optical amplifiers. *IEE Proceedings Journal*, 132(1), pp.58-63.
- Balkan, N., Serpengüzel, A., O'Brien-Davies, A., Sökmen, I., Hepburn, C., Potter, R., Adams, M.J. and Roberts, J.S., 2000. VCSEL structure hot electron light emitter. *Materials Science and Engineering: B*, 74(1-3), pp.96-100.
- Bjorlin, E.S., Riou, B., Abraham, P., Piprek, J., Chiu, Y.Y., Black, K.A., Keating, A. and Bowers, J.E., 2001. Long wavelength vertical-cavity semiconductor optical amplifiers. *IEEE Journal of Quantum Electronics*, 37(2), pp.274-281.
- Bjorlin, E.S., 2002. Long-wavelength Vertical-cavity Semiconductor Optical Amplifiers. University of California, Santa Barbara Long-wavelength Vertical-cavity.
- Chaqmaqchee, F., Abubekr Salh, S. and Mohammed Sabri, M., 2020. Optical analysis of 1300 nm GaInNAsSb/GaAs vertical cavity semiconductor optical amplifier. *Zanco Journal of Pure and Applied Sciences*, 32(2), pp.87-92.
- Chaqmaqchee, F.A., 2021. A comparative study of electrical characterization of P-doped distributed Bragg reflectors mirrors for 1300 nm vertical cavity semiconductor optical amplifiers. *ARO-the Scientific Journal of Koya University*, 9(1), pp.89-94.
- Chaqmaqchee, F.A.I, Balkan, N. and Herrero, J.M., 2012. Top-Hat HELLIISH-VCSEA for optical amplification and wavelength conversion for 0.85 to 1.3 μ m operation. *Nanoscale Research Letters*, 7(525), pp.1-6.
- Chaqmaqchee, F.A.I. and Balkan, N., 2012. Gain studies of 1.3- μ m dilute nitride HELLIISH-VCSEA for optical communications. *Nanoscale Research Letters*, 7(1), pp.1-4.
- Chaqmaqchee, F.A.I. and Lott, J.A., 2020. Impact of oxide aperture diameter on optical output power, spectral emission, and bandwidth for 980 nm VCSELS. *OSA Continuum*, 3(9), pp.2602-2613.
- Chaqmaqchee, F.A.I., 2016. Optical design of dilute nitride quantum wells vertical cavity semiconductor optical amplifiers for communication systems. *ARO-The Scientific Journal of Koya University*, 4(1), pp.8-12.
- Chaqmaqchee, F.A.I., Mazzucato, S., Oduncuoglu, M., Balkan, N., Sun, Y., Gunes, M., Hugues, M. and Hopkinson, M., 2011. GaInNAs-based Helliish-vertical cavity semiconductor optical amplifier for 1.3 μ m operation. *Nanoscale Research Letters*, 6(1), pp.1-7.
- Erol, A., 2008. *Dilute III-V Nitride Semiconductors and Material Systems: Physics and Technology*. Springer, Berlin, Germany.
- Ghadimi, A. and Ahmadzadeh, M., 2020. Effect of variation of specifications of quantum well and contact length on performance of InP-based Vertical Cavity Surface Emitting Laser (VCSEL). *Journal of Optoelectronic Nanostructures*, 5(1), pp.19-34.
- Gönül, B., Köksal, K. and Bakır, E., 2007. A theoretical investigation of carrier and optical mode confinement in GaInNAs QWs on GaAs and InP substrates. *Physica Status Solidi C*, 4(2), pp.671-673.
- Hepburn, C.J., Wah, J.Y., Boland Thoms, A. and Balkan, N., 2005. GaInNAs and GaAs, top-hat vertical-cavity semiconductor optical amplifier (VCSEA) based on longitudinal current transport. *Physica Status Solidi (c)*, 2(8), pp.3096-3099.
- Kimura, T., Bjorlin, S., Piprek, J. and Bowers, J.E., 2003. High-temperature characteristics and tunability of long-wavelength vertical-cavity semiconductor optical amplifiers. *IEEE Photonics Technology Letters*, 15(11), pp.1501-1503.
- Lee, Q.Y., Chou, C.J., Lee, M.X. and Lee, Y.C., 2022. Detecting the knowledge domains of compound semiconductors. *Micromachines*, 13(3), p.476.
- O'brien, A., Balkan, N., Boland-Thoms, A., Adams, M., Bek, A., Serpengüzel, A., Aydinli, A. and Roberts, J., 1999. Super-radiant surface emission from a quasi-cavity hot electron light emitter. *Optical and Quantum Electronics*, 31(2), pp.183-190.
- Piprek, J., Bjorlin, E.S. and Bowers, J.E., 2001. Modeling and optimization of vertical-cavity semiconductor laser amplifiers. In *Physics and Simulation of Optoelectronic Devices IX*, 4283, pp.129-138.
- Potter, R.J. and Balkan, N., 2004. Optical properties of GaNAs and GaInAsN quantum wells. *Journal of Physics: Condensed Matter*, 16(31), p.S3387.
- Razeghi, M., 2000. Optoelectronic devices based on III-V compound semiconductors which have made a major scientific and technological impact in the past 20 years. *IEEE Journal of Selected Topics in Quantum Electronics*, 6(6), pp.1344-1354
- Royo, P., Koda, R. and Coldren, L.A., 2002. Vertical cavity semiconductor optical amplifiers: Comparison of Fabry-Perot and rate equation approaches. *IEEE Journal of Quantum Electronics*, 38(3), pp.279-284.
- Su, S.T., Tang, S.F., Chen, T.C., Chiang, C.D., Yang, S.T. and Su, W.K., 2006. Temperature dependent VCSEL optical characteristics based on graded Al_xGa_{1-x}As/GaAs distributed Bragg reflectors: Reflectivity and beam profile analyses. In *Vertical-Cavity Surface-Emitting Lasers X*, 6132, pp.165-174.
- Uesugi, K., Morooka, N. and Suemune, I., 1999. Reexamination of N composition dependence of coherently grown GaNAs band gap energy with high-resolution x-ray diffraction mapping measurements. *Applied Physics Letters*, 74(9), pp.1254-1256.
- Ungan, F., Yesilgul, U., Sakiroglu, S., Kasapoglu, E., Sari, H. and Sökmen, I., 2013. Nonlinear optical absorption and refractive index in GaInNAs/GaAs double quantum wells under intense laser field and applied electric field. *Journal of Luminescence*, 143, pp.75-80.
- Wah, J.Y. and Balkan, N., 2004. Low field operation of hot electron light emitting devices: Quasi-flat-band model. *IEE Proceedings-Optoelectronics*, 151(6), pp.482-485.
- Walukiewicz, W., Shan, W., Ager, J.W. 3rd, Chamberlin, D.R., Haller, E.E., Geisz, J.F., Friedman, D.J., Olson, J.M. and Kurtz, S.R., 1999. *Nitrogen-induced Modification of the Electronic Structure of Group III-NV Alloys*. National Renewable Energy Lab.(NREL), Golden, CO, pp.520-29583.
- Yu, K.M., Walukiewicz, W., Shan, W., Wu, J., Beeman, J.W., Ager, J.W., Haller, E.E. and Ridgway, M.C., 2000. *Synthesis of III-N x-V 1-x Thin Films by N Ion Implantation*. MRS Online Proceedings Library (OPL), Germany, p.647.
- Zhao, X., Palinginis, P., Pesala, B., Chang-Hasnain, C.J. and Hemmer, P., 2005. Tunable ultraslow light in vertical-cavity surface-emitting laser amplifier. *Optics Express*, 13(20), pp.7899-7904.